

# Low-group-velocity and low-dispersion slow light in photonic crystal waveguides

Shousaku Kubo,\* Daisuke Mori, and Toshihiko Baba

Department of Electrical and Computer Engineering, Yokohama National University, 79-5 Tokiwadai, Hodogaya-ku, Yokohama 240-8501, Japan

\*Corresponding author: d06gd126@ynu.ac.jp

Received July 17, 2007; revised August 29, 2007; accepted September 6, 2007;  
posted September 10, 2007 (Doc. ID 85390); published October 8, 2007

Photonic crystal slab line defect waveguides with slightly small innermost holes are theoretically expected to show light transmission with low-group-velocity and low-dispersion (LVL) characteristics owing to a linear and almost flat photonic band. In this study, the LVL characteristics of such waveguides were experimentally confirmed by using modulation phase shift measurement and transmission of ultrashort optical pulses. These results will be applicable to buffering and nonlinearity enhancement of optical signals. © 2007 Optical Society of America

OCIS codes: 230.5298, 230.7370.

Light whose group velocity  $v_g$  is markedly slowed down in comparison with  $c$ , the velocity of light in vacuum, is called “slow light.” It is believed that slow light may find application in compact optical delay lines and optical buffers. It is also expected to enhance nonlinear effects because the optical signals are spatially compressed and their internal intensity is enhanced by the low  $v_g$ . Thus far, large material dispersion and structural dispersion have been studied to generate slow light. Photonic crystal waveguides (PCWs) consisting of a line defect in a two-dimensional (2D) photonic crystal slab show a low  $v_g$  converging to zero and a correspondingly large group index  $n_g \equiv c/v_g$  diverging to infinity owing to the large first-order structural dispersion  $dk/d\omega$  at the photonic band edge [1–3]. However, the bandwidth of slow light becomes narrower as  $v_g$  approaches zero [4]. Moreover, the waveform of high-speed optical signals is severely distorted by the large second-order dispersion (group-velocity dispersion  $d(dk/d\omega)^{-1}/d\omega$ , GVD) of slow light. To obtain useful slow light, we have proposed a directional coupler [5] and coupled waveguides [6], in which the bandwidth of slow light is expanded by a chirped structure and the GVD is internally compensated. However, these devices generally have complex structures that are difficult to fabricate. Moreover, optical signals are first dispersed and then recovered by the dispersion compensation in the device. This process is not necessarily suitable for the enhancement of nonlinear effects. In addition, the low-group-velocity and low-GVD (LVL) characteristics of PCWs have also been studied as alternative useful slow light [7,8]. A LVL PCW has a slightly modified structure from a standard PCW and shows a linear and almost flat photonic band of the main propagation mode in a particular bandwidth. For instance, when the width of the line defect is narrowed, the hole diameter  $2r$  is enlarged, the diameter  $2r'$  of the innermost holes is reduced, or the refractive index of the line defect is locally increased, the photonic band of the propagation mode approaches that of the slab mode, and weak anticrossing occurs, resulting in a linear photo-

nic band near the band edge. However, the appearance of such LVL characteristics is sensitive to these parameters, and thus a careful experiment is necessary for observation and evaluation. Recently, several experiments on LVL characteristics have been reported [9,10], but their agreement with theoretical results remains unclear. In this study, we observed the LVL characteristics of PCWs with reduced  $2r'$  [see Fig. 1(a)] by measuring the delay time using the modulation phase shift method and carefully evaluated the correspondence to theoretical results. We also confirmed the low GVD through transmission measurement of ultrashort optical pulses.

In this study, a photonic crystal slab consisting of circular holes (diameter  $2r$ ) in a triangular lattice (lattice constant  $a$ ) is assumed as the basic structure. Figure 1(b) shows the photonic band of the main propagation mode of the single-line-defect PCW when the polarization is assumed to be transverse electric. We performed a 2D analysis with an equivalent index of the slab of 2.9 because the three-dimensional (3D) calculation of band frequencies, which is precise enough to estimate  $v_g$  in the slow light regime, is very time consuming. As  $2r'/2r$  is reduced, the band shifts to lower frequencies, changing its shape from downfacing, to linear, and then to upfacing. This change is

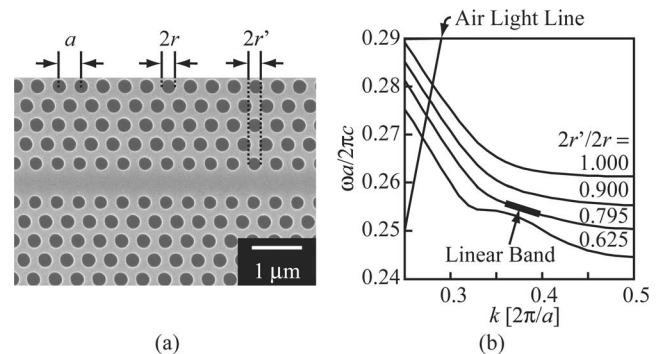


Fig. 1. Device structure and photonic band. (a) Top view of LVL PCW fabricated on SOI substrate. (b) Photonic band of the main propagation mode of PCW for  $2r/a=0.667$ .  $2r'/2r$  is taken as a parameter.

caused by the slab mode band below the propagation mode band, although it is omitted in Fig. 1(b). As can be seen from Fig. 1(b),  $2r'$  must be precisely controlled to obtain the linear photonic band, and the bandwidth of the linear section is uniquely determined. Figure 2(a) shows the group index  $n_g$  characteristics obtained from the photonic bands. A simple increase in  $n_g$  is observed for  $2r'/2r=1$ , while a step-like behavior is found in the range  $2r'/2r<0.8$  and ideal LVLD characteristics are observed for  $2r'/2r=0.795$ . The optimum  $2r'/2r$  for the LVLD also depends on  $2r/a$  because the slab mode band is shifted by  $2r/a$ . Figure 2(b) shows the  $n_g$  characteristics when  $2r/a$  is changed and  $2r'/2r$  is optimized accordingly. As  $2r/a$  is increased, the optimum  $2r'/2r$  approaches unity, and the LVLD appears at higher frequencies, exhibiting a larger  $n_g$  and narrower bandwidth:  $n_g=45$  and the normalized bandwidth  $\Delta\omega/\omega=0.4\%$  for  $2r/a=0.765$ , and  $n_g=17$  and  $\Delta\omega/\omega=1.4\%$  for  $2r/a=0.667$ . One can choose the high  $n_g$  and narrow bandwidth or low  $n_g$  and wide bandwidth according to the application. Note that there is a quantitative difference in  $n_g$  and  $\Delta\omega/\omega$  between the 2D analysis and actual 3D structures. Nevertheless, we can expect a qualitative agreement. Since photonic bands in the 3D analysis usually tend to be flatter than the 2D photonic bands, the actual  $n_g$  and  $\Delta\omega/\omega$  values will be slightly larger and narrower, respectively.

For the fabrication, a smart-cut silicon-on-insulator (SOI) substrate having a  $0.213\ \mu\text{m}$  thick top Si layer was used. A triangular lattice hole pattern with  $2r/a\cong 0.65$  was formed by electron-beam lithography and  $\text{SF}_6$  inductively coupled plasma etching. The input and output ends of the PCW were

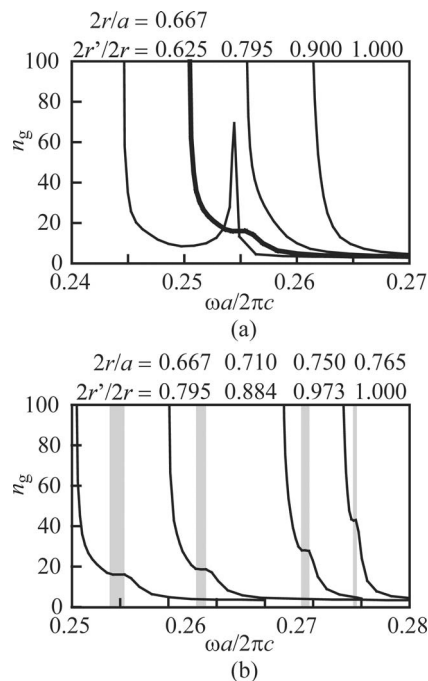


Fig. 2. Group index  $n_g$  characteristics of PCW. (a)  $2r/a$  is fixed to 0.667 and  $2r'/2r$  is varied. (b)  $2r/a$  is varied and  $2r'/2r$  is optimized to obtain the LVLD characteristics.

formed by cleavage, and the air-bridge structure was formed by HF wet etching. The diameter  $2r'$  was fine-tuned by adjusting the exposure time of the e-beam lithography. The transmission spectrum of the PCW was measured by inserting a tunable laser light, and  $n_g$  was evaluated by the modulation phase shift method using an optical network analyzer (Advantest Q7750). Figure 3 shows the results and the band diagram obtained from the above analysis (dashed curve) and from the experimental  $n_g$  using the relation  $n_g=c\Delta\omega/\Delta k$  (solid curve). When  $2r'/2r$  was decreased below unity, the drop in the transmission intensity near the band edge became more gradual. This is thought to be due to the increased coupling loss and propagation loss of the slow light whose bandwidth was expanded. Accordingly, the behavior of  $n_g$  became steplike, and LVLD characteristics appeared. When  $2r'/2r=0.89$ ,  $n_g=37$  for  $\Delta\omega/\omega=0.3\%$ . When  $2r'/2r=0.86$ ,  $n_g=30$  for  $\Delta\omega/\omega=0.7\%$ . These results qualitatively agree with the above theoretical considerations. The position of the air light line can be determined from the attenuation in transmission on the higher frequency side. The theoretical photonic band was slightly shifted so that the position of the light line agrees with the experimental photonic band. In addition, the calculation parameters were appropriately changed. Thus, the behavior of  $n_g$  and of the photonic bands corresponded approximately to the experimental results.

To confirm the low GVD, we performed transmission measurements of ultrashort optical pulses. We used a mode-locked tunable fiber laser emitting C-band optical pulses, each having a full width at half-maximum of 0.8 ps and a corresponding spectral width of 6.5 nm. The LVLD PCW sample used had a slightly small  $2r/a=0.64$  and  $2r'/2r=0.84$  and exhibited LVLD characteristic in the C-band with  $n_g=20$ . Figure 4 shows the  $n_g$  characteristics and autocorrelation traces of the input and output pulses. Arrows indicate the center wavelengths of the pulse spectrum. At  $\lambda=1.528\ \mu\text{m}$ , exhibiting a constant  $n_g$ , the width of the output pulse was almost the same as that of the input pulse. At  $\lambda=1.534\ \mu\text{m}$ , exhibiting a larger dispersion, the pulse was clearly expanded and weakened.

In summary, we theoretically investigated and experimentally demonstrated the LVLD characteristics arising from the linear photonic band in a photonic crystal line defect waveguide. By adjusting the diameters of the holes ( $2r$ ) and innermost holes ( $2r'$ ), the group index  $n_g$  and normalized bandwidth  $\Delta\omega/\omega$  of the LVLD characteristics can be controlled. When  $2r'/2r$  was reduced slightly below unity,  $n_g=30-37$  for  $\Delta\omega/\omega=0.7\%-0.3\%$ , respectively, and the LVLD characteristics corresponded approximately to those obtained by the photonic band analysis. To confirm the low GVD, subpicosecond optical pulses were inserted; no degradation was observed in the waveform of the resultant output pulses. Such slow light with LVLD characteristics is particularly effective in enhancing the internal light intensity and nonlinear effects.

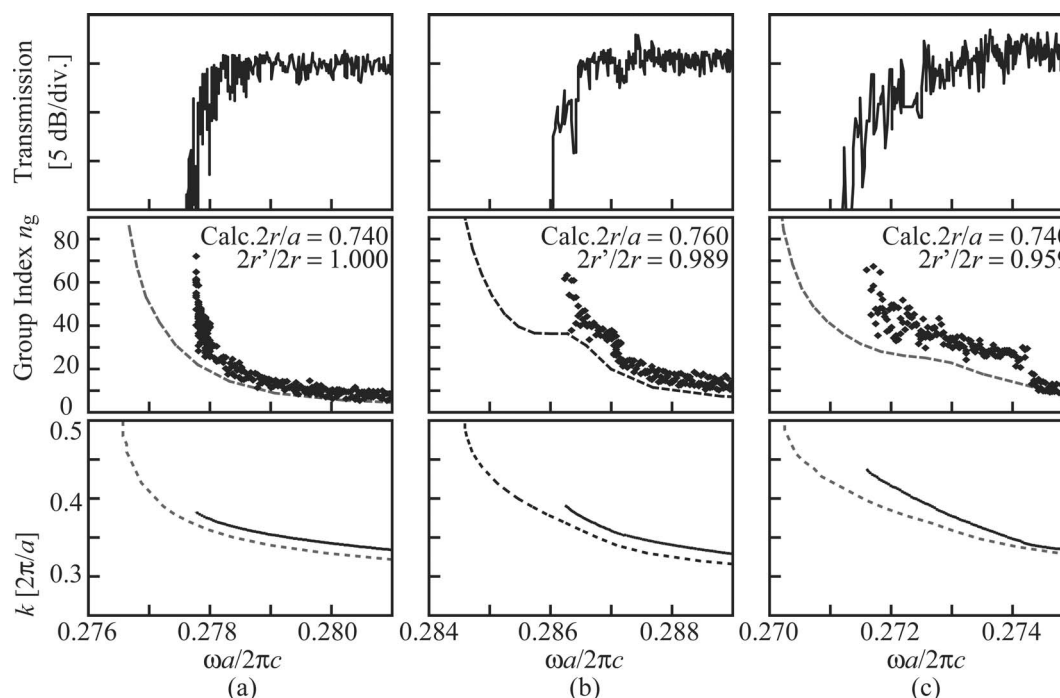


Fig. 3. Measured transmission spectrum,  $n_g$  characteristics, and band diagram experimentally evaluated for  $2r/a=0.65$  (solid curve) and calculated for the parameters in the figures (dashed curve).  $2r'/2r$  is (a) 1.00, (b) 0.89, (c) 0.86.

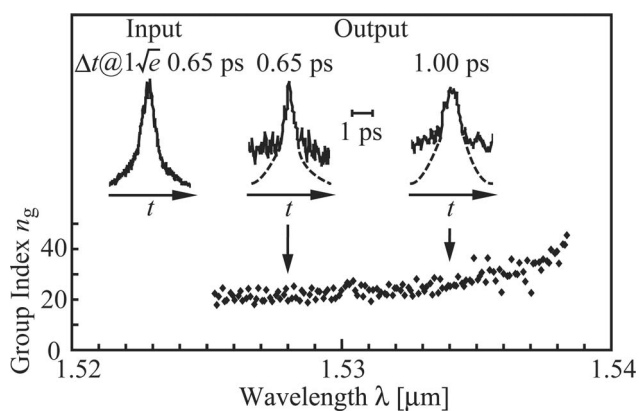


Fig. 4. Group index  $n_g$  characteristics for another sample ( $2r/a=0.64$ ,  $2r'/2r=0.84$ ) showing LVL characteristics and autocorrelation traces of input and output optical pulses.

This work was supported by the Core Research for Evolutional Science and Technology (CREST) Project of Japan Science and Technology (JST), a Grant-in-Aid for "Priority Research" from the Ministry of Education, Culture, Sports, Science and Technology (MEXT), the Telecommunications Advancement

Foundation, Support Center for Advanced Telecommunications Technology Research, and the Kurata Memorial Hitachi Science and Technology Foundation.

## References

1. M. Notomi, K. Yamada, A. Shinya, J. Takahashi, C. Takahashi, and I. Yokohama, *Phys. Rev. Lett.* **94**, 073903 (2001).
2. T. Asano, K. Kiyota, D. Kumamoto, B. S. Song, and S. Noda, *Appl. Phys. Lett.* **84**, 4690 (2004).
3. Y. A. Vlasov, M. O'Boyle, H. F. Hamann, and S. J. McNab, *Nature* **438**, 65 (2005).
4. T. Baba and D. Mori, *J. Phys. D* **40**, 2659 (2007).
5. D. Mori, S. Kubo, H. Sasaki, and T. Baba, *Opt. Express* **15**, 5264 (2007).
6. D. Mori and T. Baba, *Opt. Express* **13**, 9398 (2005).
7. A. Sakai, I. Kato, D. Mori, and T. Baba, in *17th Annual Meeting of the IEEE Laser & Electro-optics Society (IEEE/LEOS, 2004)*, paper IThQ5.
8. A. Y. Petrov and M. Eich, *Appl. Phys. Lett.* **85**, 4866 (2004).
9. L. H. Frandsen, A. V. Lavrinenko, J. Fage-Pedersen, and P. I. Borel, *Opt. Lett.* **14**, 9444 (2006).
10. M. D. Settle, R. J. P. Engelen, M. Salib, A. Michaeli, L. Kuipers, and T. F. Krauss, *Opt. Express* **15**, 219 (2007).